Biofilm Formation and Chemostat Dynamics: Pure and Mixed Culture Considerations

James D. Bryers
Swiss Federal Institute for Water Resources and Water Pollution Control, EAWAG/ETH, Swiss Federal Institute of Technology, CH-8600 Dübendorf, Switzerland

Accepted for Publication December 30, 1983

Time-dependent biofilm formation effects on continuous fermenter operation are modelled here in general for a mixed culture of N different microorganisms growing on a single substrate. Dynamic computer solutions are detailed for two versions of the general model: a pure culture and a simple two-cell mixed culture. Pure culture model predictions compare favorably with two pure culture experiments in the literature where significant biofilm formation was noted. A mixed culture of one microbe (C_1) having a higher growth rate than a second microbe (C_2) is simulated for two hypothetical scenarios of microbe C_2 having different magnitudes of cell deposition rate. Biofilm effects on the estimation of kinetic and stoichiometric parameters in both model versions, plus the impact of biofilms on mixed culture dynamics, are discussed.

INTRODUCTION

Biofilms—adherent microorganisms often entrapped within an extracellular polymeric matrix—can develop on any surface exposed to an active microbial culture. Biofilms within fermenters can create such problems as: 1) erratic effluent biomass concentrations, 2) obscure continuous culture washout, 3) atypical ecological niches within the reactor, and 4) physical fouling of reactor internals (e.g., impellers, baffles, heat exchange surfaces, pH probes, and DO probes). Despite an increasing awareness of biofilm formation and its associated detrimental effects, biofilm formation in a chemostat is often considered only a mere operating nuisance. In the interpretation of resultant chemostat data, the subtle effects of biofilms are all too often ignored; such neglect can produce inaccurate estimates of kinetic/stoichiometric parameters and can lead to erroneous conclusions about the ecological dynamics of mixed cultures.

Historically, the effects of biofilm formation on fermenter operation were not considered until 1964,[1,2] even though the effects of microbial attachment on apparent microbial activity were noted in 1943.[3] Topiwala and Hamer[4] first quantified the effects of a constant biofilm amount on the steady-state substrate and suspended biomass concentrations in a chemostat. This classical note predicted the extension (or elimination) of culture washout as a function of the assumed constant biofilm amount. The Topiwala-Hamer model (THM) was derived for pure cultures with constant kinetic/stoichiometric parameters equal for both attached and suspended microorganisms; no mass transfer limitations were considered.

Wilkinson and Hamer[5] experimentally verified the THM in continuous mixed culture studies where maximum biofilm thickness was reported at ca. 700 μm. Biofilm research increased dramatically during the seventies with most theoretical efforts directed toward modelling substrate mass transfer and biological reaction within a biofilm of constant thickness. Grady[6] provides an excellent review of such biofilm-substrate kinetic models. Characklis and colleagues[7-10] present the only comprehensive studies (both experimental and mathematical) of biofilm accumulation in chemostats; regrettably biofilm formation was carried out at constant dilution rate(s), far in excess of the culture washout. Finally, Baltzis and Fredrickson[11] extend the THM to competition between two different microbial populations for one limiting substrate where one population forms an attached monolayer (not a strict biofilm). Their study is entirely theoretical, presenting steady-state stability analysis of the system equations without experimental verification.

One purpose of this article is to present a simple general unsteady state model for biofilm formation within a continuous mixed culture system. For verification, predictions of a pure culture limiting case of the model are compared to existing literature data. Then the dynamics of a simple two-species mixed culture biofilm are considered as a function of reactor operating parameters. The second, perhaps more important purpose of this article is to clarify how a chemostat behaves when biofilm formation occurs and how to correctly interpret data resulting from such systems.

Biotechnology and Bioengineering, Vol. XXVI, Pp. 948-958 (1984)

CCC 0006-3592/84/080948-11$04.00

MODEL DEVELOPMENT

General Model

The mathematical description for biofilm accumulation is based upon the scenario proposed elsewhere by Characklis and co-workers.[8,9] The general mixed culture model is based upon the following assumptions:

1) The reactor is operated in the continuous flow mode and completely mixed with volume $V(L^3)$ and internal surface area $A(L^2)$.

2) Biomass concentration of the jth suspended microbe is denoted $C_j(M_x/L^3)$ with $j = 1 \ldots N$, where N is the total number of species in the mixed culture.

3) All suspended microbes form biofilms to some extent. Biomass areal concentration of the jth attached microbe is denoted $B_j(M_x/L^2)$ with $j = 1 \ldots N$.

4) Accumulation of each attached microbial species is the sum of rates of three individual processes: cellular deposition $R_j^D(M_x/L^2)$, growth rate of attached microbe $R_j^G(M_x/L^2)$, and a fraction f_j of the total biofilm removal rate $R^R(M_x/L^2)$.

5) Nonviable biofilm material (i.e., extracellular polymers or residue of cell lysis) is not modelled here. Consequently, the total biofilm areal density $M(M_x/L^2)$ is the sum of the areal concentrations of all attached microbes. Trulear[12] does present mass balances for both intra- and extracellular carbon in biofilms growing in pure culture chemostats. Also, endogenous decay processes are ignored; implications of this assumption are discussed in a later section.

6) The fraction f_j is assumed, without verification, to be equal to the weight fraction of microbe j in the biofilm; i.e., $f_j = B_j/M$. Due to assumption 5, $\Sigma_{j=1}^{N} f_j = 1.0$.

7) Nutrient feed streams to the reactor are sterile.

8) Both suspended and attached mixed cultures grow on a single growth-limiting substrate $S(M_s/L^3)$. Suspended growth rates of individual microbial species are considered Monod-like expressions of S; i.e.,

$$\mu_j C_j = \hat{\mu}_j S C_j/(K_s^j + S) \tag{1}$$

Attached microbial growth rates are identical Monod expressions using biofilm concentrations and could incorporate an effectiveness factor η to account for possible *internal* mass transfer resistances to S within the biofilm; i.e.,

$$R_j^G = \eta \mu_j B_j = \eta \hat{\mu}_j S B_j/(K_s^j + S) \tag{2}$$

External mass transfer resistances are considered negligible in most well-stirred fermenters. Pitcher[13] describes one such effectiveness factor η for Monod-like expressions as a function of a modified Thiele modulus ϕ_p where

$$\eta = \tanh \phi_p/\phi_p \tag{3}$$

and (adapted here to the specific biofilm situation),

$$\phi_p = \frac{K\left[(L^2/K_s D_e) \sum_{j=1}^{N} (\mu_j B_j/\alpha_j)\right]^{1/2}}{(1 + K)[2K - 2 \ln (1 + K)]^{1/2}} \tag{4}$$

where ρ is the biofilm volumetric density (M_x/L^3), L is the biofilm thickness (L) defined as (M/ρ), α_j is the attached microbial yield coefficient (M_x/M_s), D_e is the effective diffusivity of S in the biofilm (L^2/t), and K is equal to S/K_s.

9) Biofilm removal is due to prevailing shear stresses in the reactor which are considered constant for this article. Consequently, the rate of biofilm removal is assumed a function only of the total biofilm mass at the surface. Trulear and Characklis[9] suggested the following expression for biofilm removal rate,

$$R^R = k_R M^2/M_M \tag{5}$$

where k_R is the maximum biofilm removal rate at steady-state biofilm concentration $(1/t)$ and M_M is the steady-state maximum biofilm concentration (M_x/L^2).

10) Cellular deposition rates are assumed proportional to the surface area of the reactor unoccuppied by total biofilm and the concentration of specific suspended microbe. If M^* (M_x/L^2) is the maximum surface concentration considered attainable by deposition only, then, using a modified form of an expression suggested by Baltzis and Fredrickson,[11] the cellular deposition rate is,

$$R_j^D = k_j^D (M^* - M) C_j \tag{6}$$

where k_j^D is the deposition rate constant for jth microbe $(L^3/M_x t)$.

Given the above assumptions, the following equations describe mixed culture biofilm formation in a chemostat: The attached microbial equations, $j = 1 \rightarrow N$, are

$$dB_j/dt = R_j^D + R_j^G - f_j R^R \tag{7}$$

The total biofilm equation is

$$dM/dt = \sum_{j=1}^{N} (R_j^D + R_j^G) - R^R \tag{8}$$

The suspended microbial balances, $j = 1 \rightarrow N$, are

$$dC_j/dt = -DC_j + \mu_j C_j - R_j^D A/V + f_j R^R A/V \tag{9}$$

The limiting substrate balance is

$$dS/dt = D(S^0 - S) - \sum_{j=1}^{N} [(\mu_j C_j/Y_j) + (R_j^G A/V\alpha_j)] \tag{10}$$

where Y_j is the suspended microbial yield coefficient (M_x/M_s) and D is the reactor dilution rate $(1/t)$.

Case I: Pure Culture Conditions

Under pure culture conditions in the chemostat, $j = 1$ and the general model reduces to the three equations below.

The total biofilm equation is

$$dM/dt = k^D(M^* - M)C + \eta\hat{\mu}SM/(K_s + S) - k^R M^2/M_M \quad (11)$$

The suspended biomass balance is

$$dC/dt = -DC - k^D(M^* - M)CA/V + \hat{\mu}SC/(K_s + S) + k^R M^2 A/M_M V \quad (12)$$

The substrate balance is

$$dS/dt = D(S^0 - S) - \hat{\mu}SC/Y(K_s + S) - \eta\hat{\mu}SMA/\alpha(K_s + S)V \quad (13)$$

where $\eta = \tanh \phi_p/\phi_p$ as before but, for a single population,

$$\phi_p = K\sqrt{\mu\rho L^2/K_s\alpha D_e}/(1 + K)\sqrt{2K - 2\ln(1 + K)},$$

All other definitions remain unchanged. Note that there is no need for both attached microbial and total biofilm equations since, at $j = 1$, the total biofilm is composed of only one species. Results from an experimental chemostat study using *Pseudomonas putida*, with observed biofilm formation, will be compared in the next section to predictions obtained from eqs. (11)-(13) above.

Case II: Binary Culture Conditions

Here, $j = 1, 2$ for a binary culture and the general model reduces to the six equations below:
The biofilm microbe 1 equation is

$$dB_1/dt = k_1^D(M^* - M)C_1 + \eta\mu_1 B_1 - f_1 k^R M^2/M_M \quad (14)$$

The biofilm microbe 2 equation is

$$dB_2/dt = k_2^D(M^* - M)C_2 + \eta\mu_2 B_2 - f_2 k^R M^2/M_M \quad (15)$$

The total biofilm equation is

$$dM/dt = [(M^* - M)(k_1^D C_1 + k_2^D C_2)] + \eta(\mu_1 B_1 + \mu_2 B_2) - k^R M^2/M_M \quad (16)$$

The suspended microbe 1 balance is

$$dC_1/dt = -DC_1 - k_1^D(M^* - M)C_1 A/V + \mu_1 C_1 + f_1 k^R M^2 A/M_M V \quad (17)$$

The suspended microbe 2 balance is

$$dC_2/dt = -DC_2 - k_2^D(M^* - M)C_2 A/V + \mu_2 C_2 + f_2 k^R M^2 A/M_M V \quad (18)$$

The substrate balance is

$$dS/dt = D(S^0 - S) - \left(\frac{\mu_1 C_1}{Y_1} + \frac{\mu_2 C_2}{Y_2} + \frac{\eta\mu_1 B_1 A}{\alpha_1 V} + \frac{\eta\mu_2 B_2 A}{\alpha_2 V}\right) \quad (19)$$

where η is a function of the modified Thiele modulus ϕ_p as before, except ϕ_p is redefined as,

$$\phi_p = \frac{K\{(L^2/K_s D_e)[(\mu_1 B_1/\alpha_1) + (\mu_2 B_2/\alpha_2)]\}^{1/2}}{(1 + K)[2K - 2\ln(1 + K)]^{1/2}} \quad (20)$$

Steady and unsteady state solutions of eqs. (14)-(19), at different dilution rates for various culture conditions (e.g., $k_2^D \gg k_1^D$ at $\hat{\mu}_1 > \hat{\mu}_2$), will be presented in the next section.

RESULTS

Pure Culture Case

Molin[14] studied *Pseudomonas putida* (ATCC-111-72) in continuous culture at various dilution rates with asparagine as the sole carbon and single limiting substrate. The fermenter was inocculated at a substrate concentration of 3.0 g_s/L, operated batchwise until suspended biomass = 600 mg_x/L, then nutrient flow was started to affect a dilution rate of 0.6 h^{-1}. The dilution rate was then varied from a minimum $D = 0.1$ h^{-1} by regular increments to a maximum $D = 2.2$ h^{-1} without observing culture washout. After each dilution rate shift, the reactor was operated for a certain time period prior to sampling: 16 h for $D = 0.6$ and 0.1-0.6 h^{-1}; 7 h for $D =$ 0.8-1.1 h^{-1}; and 3 h for $D = 1.3$-2.2 h^{-1}.

Molin[14] reports considerable biofilm developed on all fermenter surfaces during the above experiments. Although biofilm formation was not continuously monitored during the experiment, the total biofilm amount at the completion of the culture was measured. Figures 1 and 2 summarize effluent biomass (as dry weight) and substrate concentrations reported by Molin[14] for constant inlet concentrations of 1.0 and 2.0 g_s/L asparagine, respectively.

Table I provides a summary of parameters required by the pure culture model (PCM), eqs. (11)-(13), to simulate the experiments of Molin. All values are directly from the original article except for the following: attached and suspended stoichiometric coefficients, saturation constants, deposition rate constants, and the surface concentration M^* due to deposition only. A relatively high value for the biofilm density of 50 mg_x/cm^3 was calculated from Molin's data of maximum biofilm mass, thickness, and reactor surface area. The reader should note, under these conditions of thickness and density, model estimates of ϕ_p indicate $\eta \cong 1.0$ and that internal mass transfer effects are negligible. Implications of neglecting internal mass transfer on the results will be discussed in a later section. Equations comprising the PCM are solved simultaneously using parameters in Table I with a dynamic simulator computer package named MIMIC.[15]

Predictions of both the steady-state THM and the dynamic PCM for effluent substrate and suspended biomass concentrations are superimposed upon "steady-

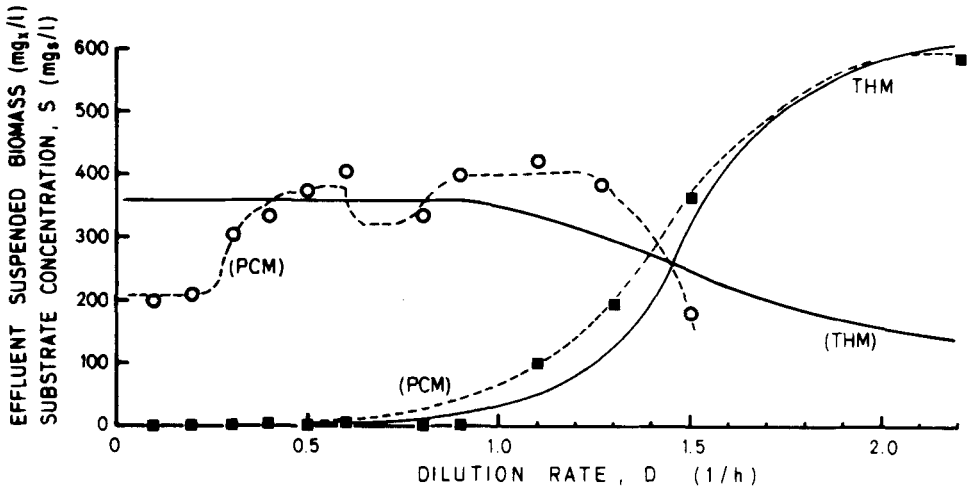

Figure 1. Steady-state (■) effluent substrate and (○) suspended cell mass reported by Molin (ref. 14) for *Pseudomonas putida* grown in chemostat culture at $S^0 = 1.0$ g_s/L asparagine. Growth conditions are given in Table I. The symbol (_____) indicates predictions of steady-state THM and (·····) indicates steady-state predictions of dynamic PCM.

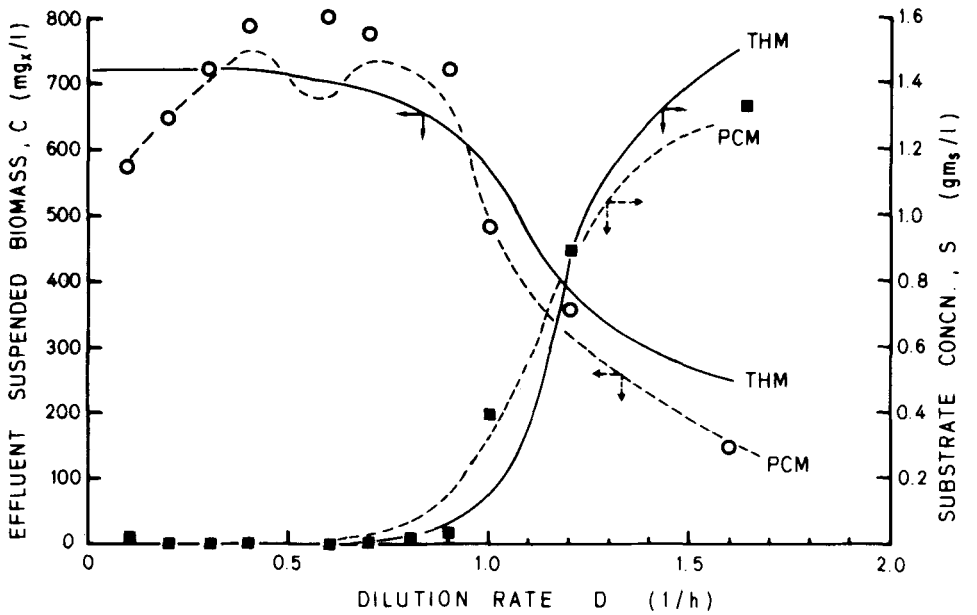

Figure 2. Steady-state (■) effluent substrate and (○) suspended cell mass reported by Molin (ref. 14) for *Pseudomonas putida* grown in chemostat culture at $S^0 = 2.0$ g_s/L asparagine. Growth conditions are given in Table I. The symbol (_____) indicates predictions of steady-state THM and (·····) indicates steady-state predictions of dynamic PCM.

Table I. Parameters used in either the dynamic pure culture model (PCM) or the steady-state Topiwala-Hamer model (THM) to simulate *Pseudomonas putida* results of Molin (ref. 14). Dilution rates varied from 0.1 to 2.2 h^{-1}.

Parameter	A[a] (cm^2)	V[a] (cm^3)	$\hat{\mu}$[a] (h^{-1})	k^R[b] (h^{-1})	k^D[c] (L/mg_x h)	K_s[c] (mg_s/L)	M_M[a] (mg_x/cm^2)	M^*[c] (mg_x/cm^2)	S^0[a] (mg_s/L)	Y and α[b] (mg_x/mg_s)
Value	800	970	0.59	0.2	3.0×10^{-5}	10.0	0.50	5.0×10^{-4}	1000 and 2000	0.32

[a] Value is taken directly from ref. 14.
[b] Value is estimated from ref. 14 data.
[c] Value is assumed.

state" data from Molin experiments 1 and 2 in Figures 1 and 2, respectively. While both models simulate overall trends in each experiment, only the PCM is able to predict the subtle variations seen in suspended biomass concentrations. Predictions of both models do not coincide at high D values, although theoretically, equations comprising the PCM will reduce to the THM under assumptions of S, C, and M at steady state. Note, however, that the PCM is a dynamic model and its predictions are dependent upon initial conditions which are determined by the previous simulation.

Biofilm formation and suspended biomass concentrations predicted via PCM for experiment 2 are illustrated in Figure 3 as a function of the time elapsed since a D value shiftup. Predicted biofilm concentrations do not attain steady state after D shifts until $D \geq 0.5\ h^{-1}$. Since effluent suspended biomass concentrations are dependent upon both suspended growth and biofilm removal processes, no true steady state in C as possible until M reaches a constant value. Consequently, at $D < 0.5\ h^{-1}$, predicted effluent suspended biomass concentrations are not at steady state and, thus, are dependent upon the time elapsed prior to sampling.

Apparent yield (Y_a) is defined traditionally for steady-state chemostats as

$$Y_a = C/(S^0 - S) \tag{21}$$

an expression which does not account for the substrate utilized for biofilm growth. In both experiments above, Y_a values increased from $Y_a \simeq 0.2\ mg_x/mg_s$ at $D = 0.1\ h^{-1}$ to $Y_a \simeq 0.40\text{-}0.45\ mg_x/mg_s$ at $D = 1.0\ h^{-1}$. Increasing yield values with increasing D are often attributed to either increasing maintenance energy requirements at the lower dilution rates or to physiological changes in the microorganisms. Tempest and Neijssel[16] proffer "apparatus effects" as a more plausible alternative to the convenient "maintenance" explanation. Illustrations above indicate that the PCM, based upon constant, equal stoichiometry for both suspended and attached growth processes, also predicts Y_a values to increase with increasing D. In these cases, Y_a increases due to the increasing (yet unaccounted for) contribution of biofilm removal processes to the suspended biomass concentration. Since biofilm removal processes are highly dependent upon shear stresses prevailing in the reactor, trends in variable Y_a with D are likely to differ between reactors operated at either different impeller speeds or fitted with a different numbers of impellers. The major error in chemostat data interpretation, when biofilm formation has not reached a steady state, is the use of eq. (21) which does not compensate for the substrate utilized for biofilm growth. Bryers[17] and Zelver[18] derive the following integral definition of yield:

$$Y = \frac{[M(t) - M(0)] + F\int_0^t C\,dt}{F\int_0^t (S^0 - S)\,dt} \tag{22}$$

directly from the steady-state version of the PCM, where F is the inlet nutrient volumetric flow rate (L^3/t). Using eq. (22), and C and S data predicted by the PCM after any dilution rate shift, $Y = 0.32\ mg_x/mg_s$, exactly the value used in the computer simulation. Under conditions

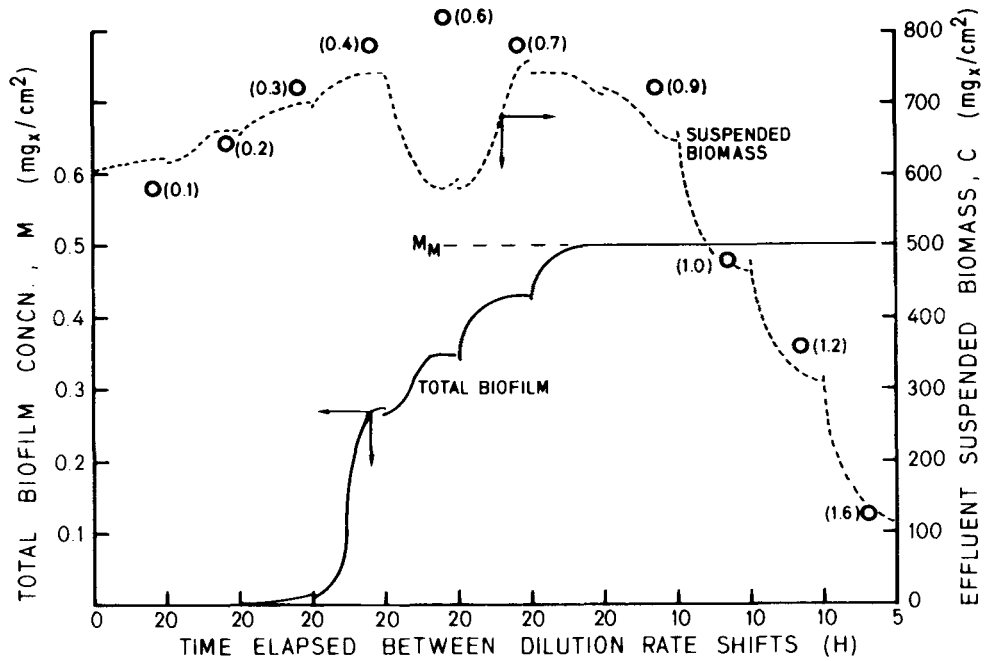

Figure 3. Predictions of PCM for transient periods after dilution rate shifts for suspended cell mass and biofilm areal concentrations. The (○) data for suspended cell mass is from Molin (ref. 14), experiment 2, with $S^0 = 2.0\ g_s/L$. Values in parentheses denote dilution rates.

of steady state with respect to S, C, and M, eq. (21) is still insufficient to estimate true stoichiometry. Assuming attached and suspended yield terms to be equal, at steady state, eq. (13) reduces to the following,

$$Y = (\mu C + \eta\mu MA/V)/D(S^0 - S) \qquad (23)$$

which does account for the biofilm's use of substrate.

Figure 4 serves to illustrate, for experiment 2 conditions, the increasing use of substrate for biofilm growth predicted by the PCM. Biofilm substrate utilization rate is shown 1) negligible early in the experiment, 2) contributing to 50% of the total substrate removal rate at $D \simeq 1.2\ h^{-1}$, and 3) reaching a maximum of 74% of the total substrate removal rate at $D = 2.2\ h^{-1}$. Although suspended biomass is unlikely to increase due to reproduction at $D > 2.0\ h^{-1}$ (residence times < 0.5 h), substrate utilization by suspended bacteria, originating due to biofilm removal, can not be considered negligible.

Simple Binary Culture Model

The illustration of biofilm effects on a mixed culture will be considered here only for a simple binary microbial culture, with both microorganisms competing, attached and suspended, for a single limiting substrate. Growth kinetics for each bacteria are depicted in Figure 5 ($\hat{\mu}_1 > \hat{\mu}_2$, $K_1^s = K_2^s$) and are selected since under ideal circumstances neither microbe 1 nor microbe 2 will coexist in a chemostat. Other mixed cultures scenarios are possible based on either different growth kinetics or on the specific microbial interactions (e.g., competition versus commensalism versus predation) selected, but such variations are not considered here.

Two hypothetical cases based upon the above kinetics are treated with the binary culture model (BCM). In both cases, the deposition rate constant of the slower growing cell 2 is greater than for cell 1: in case A, $k_2^D = 10k_1^D$ and in case B, $k_2^D = 1000k_1^D$. Other model parameters used in the BCM simulations are given in Table II. Once again, biofilm density is set equal to 50 mg_x/cm^3 which has the effect of "cultivating," computerwise, thin but reactive biofilms. At this specific density, heterogeneous biofilms would have to exceed ca. 100 μm before internal mass transfer resistances become significant. In the following hypothetical situations, biofilm thicknesses never exceed 100 μm, thus tacitly ignoring internal mass transfer effects.

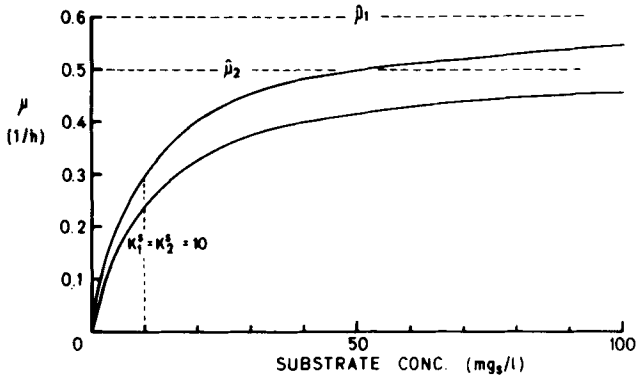

Figure 5. Growth kinetics used in binary culture model (BCM) simulations.

Table II. Model parameters used in binary culture simulations.

Parameters common to all simulations:	
A (cm^2)	1000.0
V (cm^3)	1000.0
k^R (h^{-1})	0.3
$K_1^s = K_2^s$ (mg_s/L)	10.0
M_M (mg_x/cm^2)	0.50
M^*(mg_x/cm^2)	0.0001
S^0 (mg_s/L)	500.0
Specific parameters:	
$\hat{\mu}_1$ (h^{-1})	0.60
$\hat{\mu}_2$ (h^{-1})	0.50
$Y_1 = \alpha_1$ (mg_x/mg_s)	0.30
$Y_2 = \alpha_2$ (mg_x/mg_s)	0.35
k_1^D (L/mg_x h)	3.0×10^{-5}
k_2^D (L/mg_x h)	3.0×10^{-4} (case A)
	3.0×10^{-2} (case B)
Batch initial conditions:	
$S(0) = 3000.0$ mg_s/L, $C_{1,2}(0)$ and $B_{1,2}(0) = 0.0$ mg_x/cm^2.	5.0 mg_x/L,

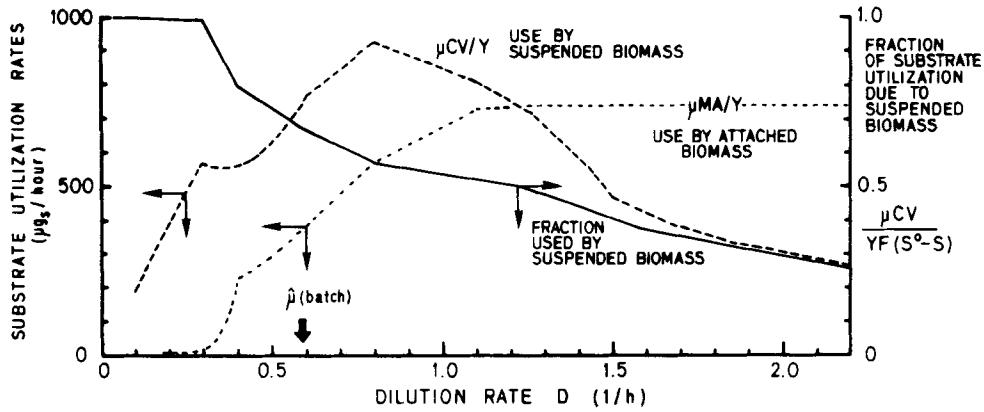

Figure 4. Relative destinations of substrate utilized as predicted by PCM for Molin experiment 2.

Both hypothetical cases, A and B, are initiated as batch reactor simulations with the batch initial conditions given in Table II. After eight hours simulated batch operation, continuous flow is initiated by setting $D = 0.1$ h^{-1}. The dilution rate is then incrementally increased from 0.1 to 6.0 h^{-1} in case A (3.0 h^{-1} for case B), modelling a chemostat experiment similar to the previous PCM analysis. The elapsed time between D shifts are as follows: 30 h for $D = 0.1$ h^{-1}, 20 h for $D = 0.2$-0.9 h^{-1}, and 10 h for $D = 1.0$-3.0 h^{-1}. Equations comprising the BCM are again solved numerically using the dynamic simulator computer package MIMIC.[15]

BCM Simulations—Case A

Case A simulates microbe 1 growing faster than microbe 2, both in suspension and in a biofilm but microbe 2 having a 10× greater deposition rate. Deposition is modelled here as microbe transport to plus attachment at the reactor surface; therefore, a higher deposition rate for one species may arise from that species' greater ability to produce either extracellular polymers or "holdfast" structures.

Steady-state effluent substrate, suspended cell concentrations (C_1 and C_2), biofilm composition (M and f_1), and apparent yield values predicted from the BCM for case A conditions are given in Figures 6 and 7.

Microbe 1 is predicted to persist in the reactor until $D = 6.0$ h^{-1} (residence time is 0.167 h or 10 min), characteristic of chemostat biofilm formation as illustrated previously for pure cultures. Not unexpectedly, microbe 1 dominates the suspended culture, although the BCM also predicts microbe 2 to remain in the reactor until $D = 6.0$ h^{-1} but at very low concentrations ($C_2 \leq 3.0$ mg_x/L). Predicted microbe 1 biofilm concentrations indicate the higher microbe 1 growth rate more than compensates for the 10× greater deposition rate of microbe 2. At $D = 1.2$ h^{-1}, microbe 1 comprises more than 90% of the

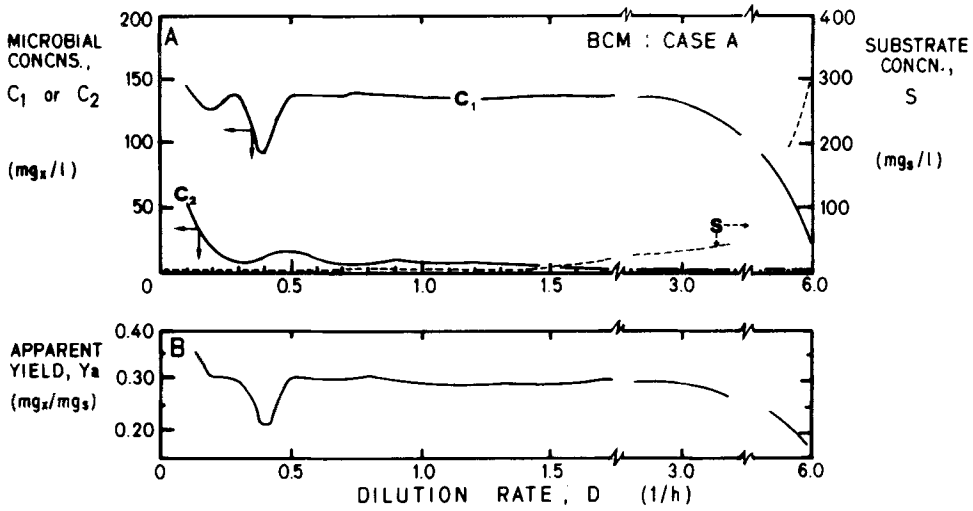

Figure 6. (a) Predictions of BCM for case A conditions (see Table II) for steady-state effluent concentrations of both microbes 1 and 2 plus limiting substrate. (b) Apparent yield values Y_a calculated using erroneous eq. (21).

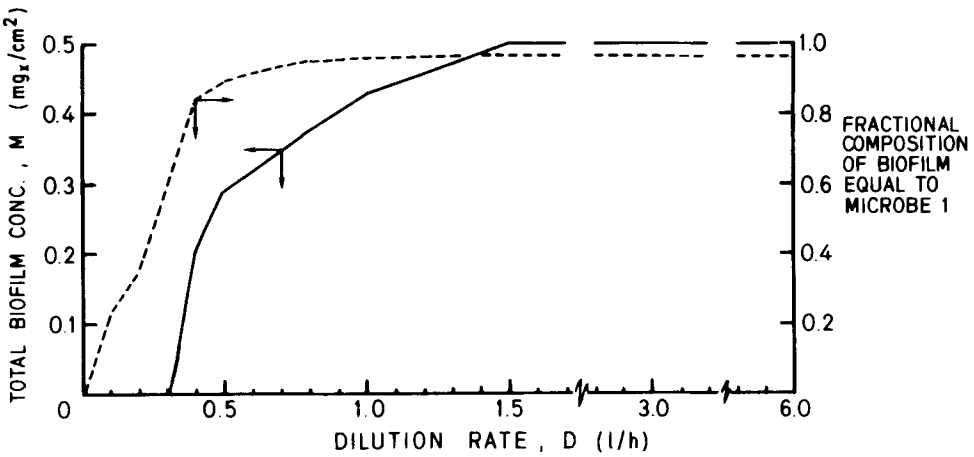

Figure 7. The BCM predictions for total biofilm concentration (M) and fraction of microbe 1 in biofilm (f_1) under case A conditions as a function of time elapsed after a dilution rate shiftup.

biofilm. Apparent yield values [Fig. 6(a)] vary during D shifts, due to changes in culture composition and the washout or dilution effect at $D = 0.4\ h^{-1}$ which is muted by increasing biofilm formation. At $D > \hat{\mu}_1$, apparent yield values equal the true stoichiometry for microbe 1 due to its predominance in the biofilm, the origin of all suspended biomass.

BCM Simulations—Case B

Case B simulates identical conditions to case A, except the deposition rate of microbe 2 is set 1000× higher than that of microbe 1. Steady-state effluent substrate concentrations, suspended microbe concentrations (C_1 and C_2), biofilm composition (M and f_1), and apparent yield values predicted by the BCM as a function of D are given in Figures 8 and 9. Figure 8(a) shows that both microorganisms again persist in the reactor until a D of 3.0 h^{-1} (mean residence time is 0.33 h or 20 min) due to biofilm formation but, unlike case A, here microbe 2, the slowest growing microorganism, predominates when $D > 0.3$ h^{-1}. Although C_1 is predicted to persist throughout the simulated experiment, C_1 concentrations after $D = 0.3$ h^{-1} never exceed 30 mg_x/L. Given the advantage of a much higher deposition rate, microbe 2 dominates the biofilm, not allowing microbe 1 to establish and take advantage of its higher growth rate.

Transient changes in microbe 1 versus microbe 2 concentrations predicted after a shiftup from $D = 0.2 \rightarrow 0.3$ h^{-1} (Fig. 10) further illustrate the dominance of microbe

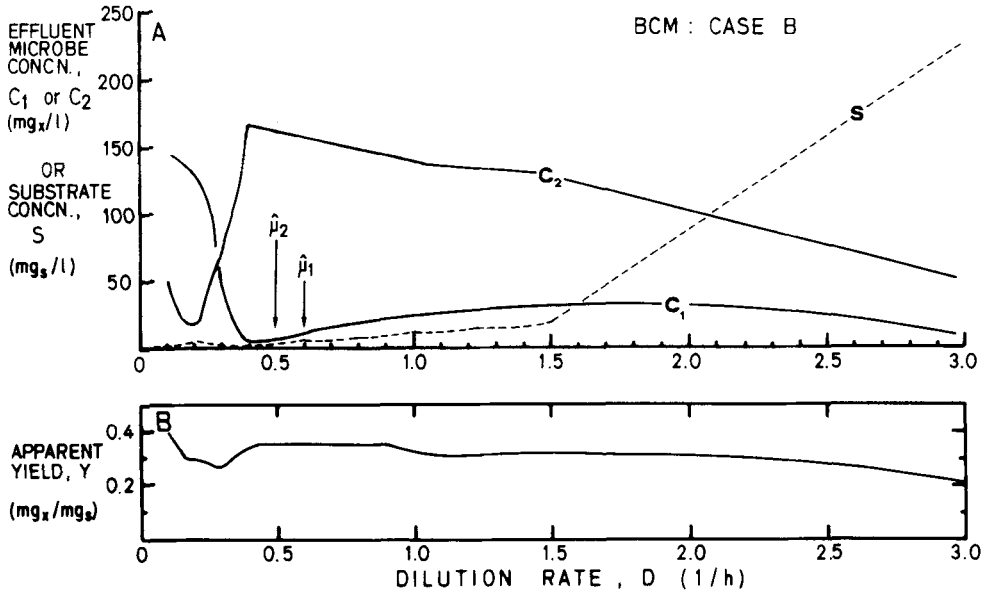

Figure 8. (a) Predictions of BCM for case B conditions (see Table II) for steady-state effluent concentrations of both microbes 1 and 2 plus limiting substrate; (b) apparent yield values (Y_a) calculated using erroneous eq. (21).

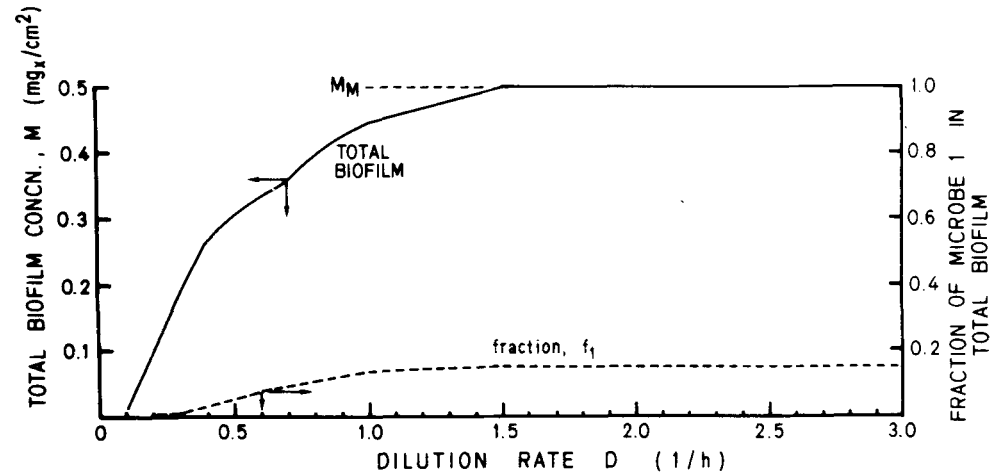

Figure 9. The BCM predictions for total biofilm concentration (M) and fraction of microbe 1 in biofilm (f_1) under case B conditions as a function of time elapsed after a dilution rate shiftup.

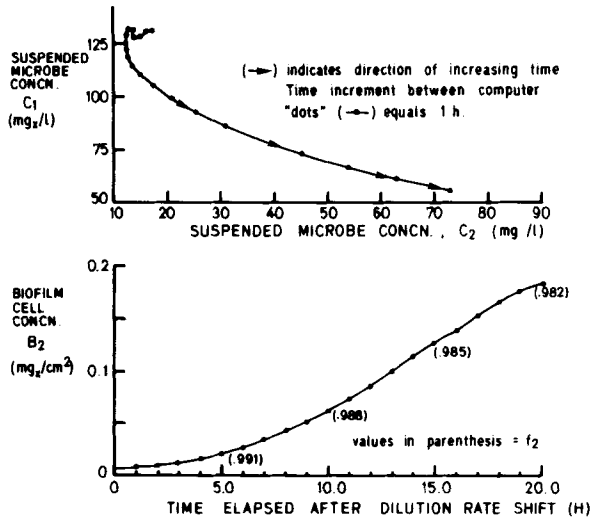

Figure 10. (a) Transient response of suspended microbes 1 and 2 concentrations and (b) biofilm B_2 cell concentrations during a dilution rate shift from $D = 0.2$ to 0.3 h^{-1}. The arrow in (a) indicates the direction of increasing elapsed time.

2 over microbe 1 due to the higher microbe 2 biofilm concentration. Apparent yield values never equal the true stoichiometry of either species except for conditions $D = 0.5$–0.8 h^{-1}, reflecting the combined influence of both biofilm microorganisms on substrate utilization. Changes in the various process rates at different stages of biofilm development are shown in Figure 11 and illustrate the dynamics of biofilm formation on chemostat operation.

Model Limitations

Two processes that are associated with biofilms—mass transfer and endogenous decay—were either implicitly or explicitly ignored in the simulations above. The impact of neglecting these fundamental processes on the above results is not trivial and warrants some discussion.

Under the simulation conditions above, internal mass transfer effects, although incorporated in the models, were tacitly ignored. External mass transfer resistances were explicitly ignored for the well mixed fermenters under consideration. However, in certain situations (e.g., plug flow reactors operated at laminar flow, slow moving or quiescent aquatic systems), external mass transfer could be significant. Under biofilm parameters (e.g., L, ρ, $\hat{\mu}$, D_e, K_s) different from those used here, the modified Thiele modulus ϕ_p could be such that the effectiveness factor $\eta \ll 1.0$.

What impact would either a finite mass transfer resistance (external or internal) or a significant endogeneous decay rate have on the results above? Several mechanisms could, alone or in combination, control the overall biofilm substrate removal rate; they are: 1) substrate mass transport to the biofilm, 2) substrate mass transport within the biofilm, and 3) simultaneous biological reaction. Substrate mass transport within the biofilm has been traditionally modelled with *molecular diffusion* only, but recent results[19] indicate *convective transport* within a biofilm can occur; however, such a novel transport mechanism will not be considered in this discussion. Rather, the effects of finite mass transfer will be qualitatively discussed for pure and mixed culture cases.

For pure culture situations, finite internal or external mass transfer resistances would effectively reduce the overall substrate removal rate of the biofilm at a certain substrate concentration. This would, in turn, reduce the biofilm development rate and the portion of the suspended biomass in the chemostat that originates as biofilm. Generally speaking, external mass transfer resistances would reduce the deviation from ideal chemostat theory created by the biofilm's presence but would also

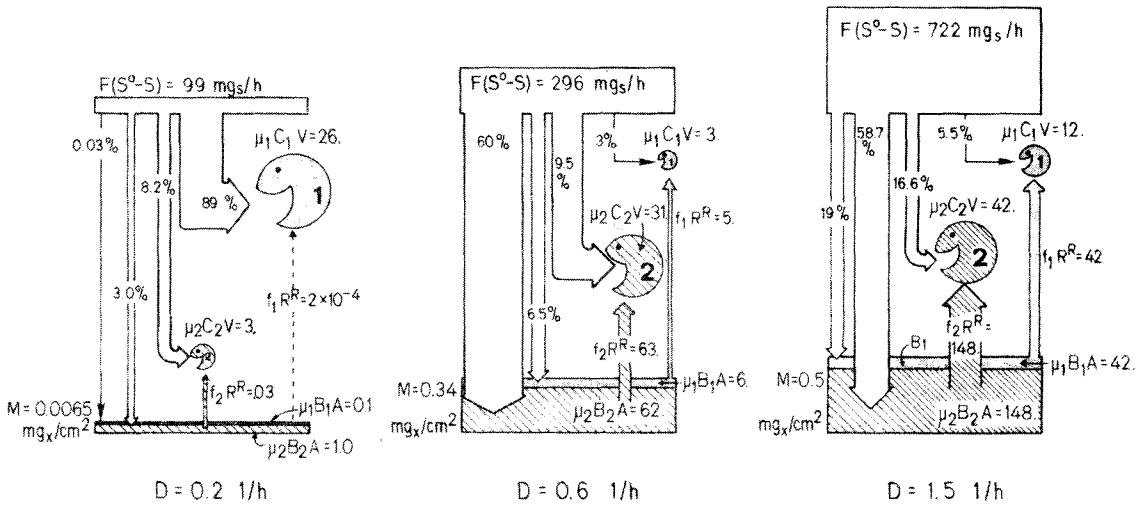

Figure 11. Process dynamics predicted by BCM at three different stages of biofilm formation under case B simulation. Unless otherwise annotated, all numerical values represent biomass production rates and have units of mg_x/h. Note that at $D = 1.5$ h^{-1}, the biofilm is constant at $M = 0.5$ mg_x/cm^2 and biofilm growth rate terms for microbes 1 and 2 equal their respective biofilm removal rates.

reduce the maximum overall substrate removal rate. Specifically, for first-order intrinsic biological reactions (i.e., $S \ll K_s$), external mass transfer does not change the apparent order of the overall substrate removal rate since both transport and reaction are first-order processes; only the apparent rate constant is changed. For zero-order kinetics (i.e., $K_s \ll S$), the observed rate is not influenced by external mass transfer.

Numerous works exist describing the effects of internal mass transfer on biofilm substrate removal rates.[6] For the pure culture case, where microorganisms are uniformly distributed throughout the biofilm, internal mass transfer effectively reduces the amount of substrate that can be removed by the biofilm, decreasing the biofilm production rate, and thus the amount of biofilm entrained into the liquid. As with external mass transfer, the general impact of internal mass transfer is to reduce the deviation caused by biofilms from ideal chemostat performance. Note that external mass transfer resistances are subject to change by engineering factors (e.g., fluid velocity) while internal mass transfer is a function of the physical and biological properties of the biofilm.

Little is known about the effects of mass transfer on mixed culture biofilms. For example, where carbon removal and nitrification are combined in a wastewater treatment fixed-film reactor, heterotrophic bacteria oxidizing organic carbon grow at markedly higher rates than the autotrophic bacteria (*Nitrosomonas* and *Nitrobacter* spp.) oxidizing NH_4^+ to NO_2^- and then to NO_3^-. Finite mass transfer resistances, predominantly internal, could foster a situation, as illustrated in Figure 12, where local bacterial turnover rates differ dramatically between species.[20,21] If the total biofilm density remains constant during growth, then the different microbial turnover rates would create spatial profiles of each group in the biofilm. In such cases, the net biofilm development rate is an integral value of the species local net biomass production rates. Biomass removal from the biofilm would be dominated by the faster growing organism that is most likely inhabiting the upper layers of the biofilm. The model derived in this article does not pretend such sophistication, and for the purposes of this article such a complex model is unnecessary.

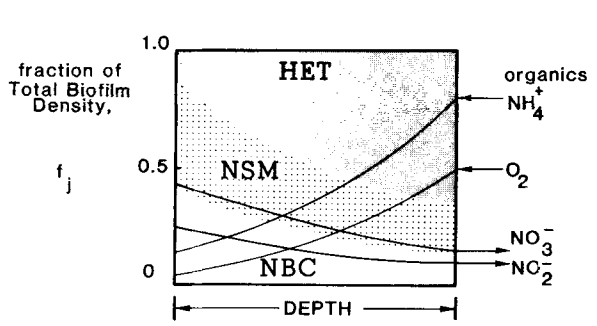

Figure 12. Hypothetical mixed culture biofilm development under the influence of internal mass transfer resistances where the growth rates of the individual microbe groups differ markedly. Illustrated is a hypothetical situation of heterotrophs (HET) oxidizing organics and autotrophs (*Nitrosomonas* = NSM and *Nitrobacter* spp. = NBC) oxidizing NH_4^+ and NO_2^-, respectively.

CONCLUDING REMARKS

Dynamic models developed here extend previous steady-state, constant biofilm models by simulating not only the extension of washout brought about by biofilm formation, but also variable yield trends more accurately. These models are simple material balances and can be easily modified to simulate various mixed culture interactions (e.g., competition, mutualism, commensalism, and predation), different suspended growth dependences (e.g., substrate or product inhibition), and various biofilm processes (internal mass transfer resistance and endogenous decay).

Implications of the above analysis of biofilm formation in a chemostat are the following:

1) Biofilm formation will bias not only $\hat{\mu}$ values as estimated from wash-out experiments but also can, if not considered, contribute to erroneous estimates of stoichiometry. Efforts to either minimize biofilm formation or, during an experiment, measure biofilm formation for use in appropriate material balances are urged. At least, an estimate of the maximum biofilm amount present at the end of an experiment would prove invaluable, as shown here, for interpreting chemostat data.

2) Estimates of stoichiometry in either pure or mixed cultures, using eq. (21), $Y_a = C/(S^0 - S)$, are wrong if biofilms occur. This equation ignores that part of the substrate used in biofilm growth, thus underestimating the true stoichiometry.

3) Effluent suspended biomass in a chemostat experiencing biofilm formation arises due to suspended growth *and* biofilm removal precesses. As the dilution rate approaches and exceeds $\hat{\mu}$, that portion of the suspended biomass due to suspended growth decreases. Although well past $\hat{\mu}$ for washout, suspended biomass from the biofilm can actually utilize substrate at a significant rate.

Note the tacit problem implied above with regard to data comparison between experiments or different systems. Biofilm removal rates are highly dependent upon prevailing shear stresses. Consequently, two identical cultures, grown at identical nutrient conditions but with slightly different hydrodynamics (i.e., impeller speed, number, and location, number of baffles, etc.), could produce different effluent concentrations.

4) Decreasing apparent yield values with decreasing growth rate (or D) may not be due to so-called maintenance requirements but can, as shown here, be attributed to biofilm formation.

5) Successive washout of different members of a mixed population will be biased under conditions with biofilm formation. Depending on a cells ability to remain at a surface and attach, a higher growth rate is not sufficient to insure dominance of one species over another.

6) Model predictions suggest biofilms can be metabolically more active (based upon total substrate uptake)

than suspended. Yet, until recently,[22] microbial activity in most natural aquatic environments has been assessed by sampling free floating microorganisms, rather than either sessile or biofilm entrapped cells. Neglecting adherent biomass may underestimate the capacity of a water system to assimilate a particular pollutant load.

References

1. D. H. Larsen and R. L. Dimmick, *J. Bacteriol.*, **88,** 1380 (1964).
2. R. J. Munson and B. A. Bridges, *J. Gen. Microbiol.*, **37,** 411 (1964).
3. C. E. Zobell, *J. Bacteriol.*, **46,** 39 (1943).
4. H. H. Topiwala and G. Hamer, *Biotechnol. Bioeng.*, **13,** 919 (1971).
5. T. Wilkinson and G. Hamer, *Biotechnol. Bioeng.*, **16,** 251 (1974).
6. C. P. L. Grady, "Modeling of Biological Fixed Films—A State of the Art Review," Proceedings of the First International Conference on Fixed Film Biological Processes, Kings Island, OH, 1982.
7. W. G. Characklis, *Biotechnol. Bioeng.*, **23,** 1923 (1981).
8. J. D. Bryers and W. G. Characklis, *Biotechnol. Bioeng.*, **24,** 2451 (1982).
9. M. G. Trulear and W. G. Characklis, *J. Water Pollut. Control Fed.*, **54,** 1288 (1982).
10. W. G. Characklis and K. E. Cooksey, *Adv. Appl. Microbiol.*, **29,** 93 (1983).
11. B. C. Baltzis and A. G. Fredrickson, *Biotechnol. Bioeng.*, **25,** 2419 (1983).
12. M. G. Trulear, "Cellular Reproduction and Extracellular Polymer Formation in the Development of Biofilms," Ph.D. dissertation, Montana State University, Bozeman, MT, 1983.
13. W. H. Pitcher, *Catal. Rev.-Sci. Eng.*, **12,** 37 (1975).
14. G. Molin, *Eur. J. Appl. Microbiol. Biotechnol.*, **13,** 102 (1981).
15. "MIMIC—A digital simulation language," Control Data Corp., Sunnyvale, CA, Ref. Manual No. 44610400, 1968.
16. D. W. Tempest and O. Neijssel, Proceedings of the Third International Symposium on Microbiology and Growth on C_1 Compounds, August, 12-16, 1980.
17. J. D. Bryers, "Dynamics of Early Biofilm Formation in a Turbulent Flow System," Ph.D. dissertation, W. M. Rice University, Houston, TX, 1980.
18. N. Zelver, "Biofilm Development and Associated Energy Losses in Water Conduits," M.S. thesis, W. M. Rice University, Houston, TX, 1979.
19. H. Siegrist and W. Gujer, unpublished.
20. J. C. Kissel, P. L. McCarty, and R. L. Street, *J. Environ. Eng.*, **110** (2), 393 (1984).
21. W. Gujer, O. Wanner, and J. D. Bryers, Swiss Federal Institute of Water Research and Water Pollution Control (EAWAG), personal communication.
23. G. G. Geesey, R. Mutch, J. W. Costerton, and R. Green, *Limnol. Oceanogr.*, **23,** 1214 (1978).